Nanobiosystems: Processing, Characterization, and Applications III,
Proc. of SPIE, vol. 8103, 810307 (1-10) (2011)

Metal incorporated M-DNA: structure, magnetism, optical absorption

Kenji Mizoguchi

Department of Physics, Tokyo Metropolitan University, Minamiosawa Hachioji, Tokyo, 192-0397 Japan;

ABSTRACT

DNA is an interesting material from the viewpoint of the materials science. This paper discusses the electronic states of the metal incorporated M-DNA complexes with several species of metal ions. M-DNA prepared by the ordinary methanol precipitation technique has been investigated with ESR, STM and optical absorption, and concluded that the metal ion hydrated with several water molecules locates in between the bases of a base pair and that the divalent metal ions are incorporated into DNA in place of two Na cations as the counter ion for PO_4^- in the DNA backbones. Only in Fe-DNA, it was confirmed that the Fe^{2+} in the $FeCl_2$ aqueous solution reacts with DNA to form Fe-DNA complex with Fe^{3+}, where the charge would transfer to DNA. Within 30 min, the hydrolysis of Fe^{2+} to form $Fe^{3+}O(OH)$ did not occur in the $FeCl_2$ aqueous solution at room temperature. The optical absorption spectra of Fe-DNA is similar to that for $FeCl_3$ with the ionic character, but definitely differs from that of $Fe^{3+}O(OH)$ with the covalent bonding nature, suggesting the ionic character of Fe^{3+} in Fe-DNA. Finally, the possible two kinds of electronic states for Zn-DNA with different bonding nature will be discussed in relation to the recent report on Zn-DNA.

Keywords: DNA, charge transfer, divalent metal ion, magnetic susceptibility, ESR, optical absorption, STM

1. INTRODUCTION

As a container of genes, a vast number of researches on deoxyribonucleic acid (DNA) have been reported, so far, since the double helical structure was found in 1953 by Watson, Click, Wilkins and Franklin.[1–4] On the other hand, the physical properties, such as electrical and magnetic properties of pristine DNA (abbreviated as B-DNA) has also attracted our attention as one of the prospective materials for the nanotechnologies,[5–16] because of excellent ability of DNA in self-organization and designing, based on the complementation of the base pairing. The diverse conclusions, however, were reported in the electrical properties; metallic,[5] semiconducting,[6,8] vicinity effect of the Cooper pair in superconductor,[10] insulating.[11] The possible origins of these discrepancies with direct measurements of DNA double helix or DNA bundles would be due to salt residue, effective doping, for example, caused by electron bombardment of TEM, interaction with substrates and so on. At least in B-DNA a consensus has been reached on this issue that B-DNA is of semiconducting with the energy gap more than 4 eV on the basis of transport, optical, magnetic and theoretical investigations.[7–9,11,17–19]

Thus, it is interesting for us to introduce the charge carriers into DNA from the viewpoint of nanotechnological application of DNA. Lee and coworkers reported a cooperative conformational change of DNA with divalent metal ions in 1993.[20] They proposed that the metal ions locate in between the bases of a base pair, as shown schematically in Fig. 1, from disappearance of the ^{1}H-NMR peaks corresponding to the hydrogen bondings connecting the bases.[20] This model is widely supported by NMR,[20] ESR[18,21–24] and IR analysis.[25] In 2001, Rakitin and coworkers suggested that DNA incorporated with Zn^{2+} could show a metallic transport nature.[15,26] Alexandre and coworkers[27] theoretically suggested the electronic states with the reduced energy gaps strongly dependent on the metal ion species for Zn^{2+}, Co^{2+} and Fe^{2+}. The magnetic studies on M-DNA with divalent metal ions, M=Ca, Mg, Mn, Co, Ni, Zn reported absence of the charge transfer from M to DNA bases, which suggests the energy gap keeps alive.[18,21–24] Very recently, on the contrary, Omerzu and coworkers have reported that Pauli-like magnetic susceptibility was observed in the specially prepared sample of dry, fluffy material as a mixture of Tris-HCl, $ZnCl_2$ and Zn^{2+}-DNA.[28] The conclusion is extremely interesting, but it is required to

Further author information: E-mail: mizoguchi@phys.se.tmu.ac.jp

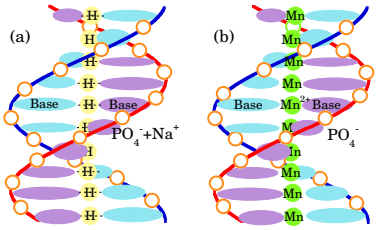

Figure 1. The schematic double helix structure of B-form DNA and Mn^{2+} ion inserted Mn-DNA. Lee and coworkers have proposed that metal ions are incorporated in between the bases of a base pair, instead of the hydrogen bonds.[20]

reexamine to resolve what is the spin carriers in Zn-DNA, where the valence of Zn has been confirmed to be Zn^{2+}, demonstrating the absence of charge transfer from Zn to DNA.[28] Another interesting fact is that Fe^{2+} ion incorporated DNA transforms to Fe^{3+}, as evidenced by the ESR g-shift around the free electron g-value, the magnetization curves and the color change from weak greenish to light ocher, suggesting the electron transfer from Fe to bases.[21]

In this report, a magnetic study with mainly ESR and SQUID, a structural study with STM and an optical absorption study will be reviewed on M-DNA incorporated with divalent metal ions, to unveil the electronic states of M-DNA, on the basis of the reported works in Refs.18, 21–24, 29, 30

2. EXPERIMENTAL

Salmon DNA in a form of fiber was provided by Wako Pure Chemical Industries, Ltd. and the Ogata Materials Science Lab., and oligo-DNA from Hokkaido System Science. M-DNA was prepared from the 1 mmol/L aqueous solution of DNA, mixed with the 5 to 10 mmol/L aqueous solution of MCl_2 (M = Mg, Ca, Mn, Fe, Co, Ni, Zn). Here, note that MCl_3 with M^{3+} did not form M-DNA composite. After stirring for 10 - 30 min, excess cold ethanol at -20 °C is poured into the transparent DNA-MCl_2 solution resulting in transparent precipitate for M-DNA, except for light pink/purple for Co-DNA, greenish for Ni-DNA and light ocher color for Fe-DNA. The residual MCl_2 is washed out thoroughly from the obtained precipitate in pure ethanol where DNA and M-DNA is insoluble. Thus obtained M-DNA were dried to form a film in the atmosphere. As a better way to obtain a homogeneous film, MCl_2 was removed from the mixed solution of M-DNA and MCl_2 with a dialyzer. The samples in the "wet" condition were saturated with water molecules at room temperature (RT) and sealed in a quartz tube for SQUID and ESR measurements. The "dry" samples were evacuated for one hour or more before sealed in a quartz sample tube. It was confirmed with ^{1}H NMR that the wet DNA contains about 12 H_2O molecules per each base pair in the double helix of DNA. In the dry state, it contains still about four water molecules. Circular dichroism (CD) spectra are examined to confirm the B-form of the double helix structure of B-DNA and M-DNA solutions. X-ray fluorescence analysis indicated that the molar ratio of phosphorous and metal ion was approximately two to one as expected for the metal ion located in the center of a base pair substituted for two sodium ions compensating two phosphoric anions in DNA backbone. UV/VIS absorption spectra are measured with UV-1700 (SHIMADZU).

3. BONDING NATURE OF MN ION IN MN-DNA

The electronic states of Mn ion in Mn-DNA prepared with the conventional technique of ethanol precipitation have been unveiled with ESR study in aqueous solution of Mn-DNA.[30] In the aqueous solution of Mn-DNA, the six hyperfine split peaks caused by a $I = 5/2$ Mn nuclear spin are observed, as demonstrated in Fig. 2.

3.1 Hyperfine spilitting

The hyperfine interaction between the electrons and the nucleus of Mn ion in the unit of Gauss is expressed as[31]

$$\frac{\mathcal{H}_{hf}}{g\mu_{\rm B}} = \mathbf{I}\cdot\mathbf{A}\cdot\mathbf{S} = A_0\mathbf{I}\cdot\mathbf{S} + \mathbf{I}\cdot\mathbf{A}_{\rm ani}\cdot\mathbf{S}, \tag{1}$$

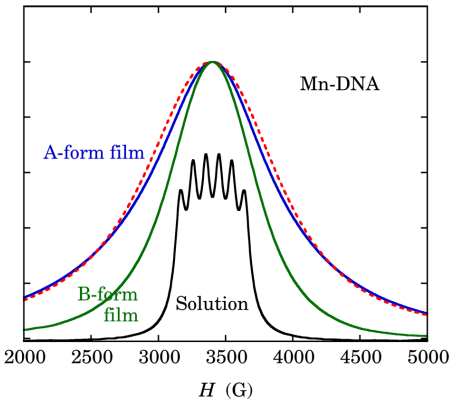

Figure 2. The absorption spectra for $(Ca_{1-x}Mn_x)$-DNA ($x = 1, 0.1, 0.01$) in solution, and B-form and A-form Mn-DNA films are shown.[30] The spectra in solution agree with each other within uncertainty. The simulation for the A-form Mn-DNA in terms of the six Lorentzian spectra with the same separation as those in solution Mn-DNA is also shown by the broken curve, which fails to reproduce the Lorentzian line shape in the A-form Mn-DNA.

where $\mathbf{I}$ is the nuclear spin and $\mathbf{S}$ is the electron spin, and $\mathbf{A}$ is the hyperfine coupling tensor, which is a sum of the isotropic part A_0 and the traceless anisotropic part $\mathbf{A}_{\rm ani}$. In Mn-DNA solution, DNA double helices are rapidly tumbling, which averages the anisotropic part $\mathbf{A}_{\rm ani}$ out at zero, giving rise to $\mathbf{A} \approx A_0$. Neglecting the small nuclear Zeeman energy, the electron spin hamiltonian for the Mn-DNA solution,

$$\frac{\mathcal{H}}{g\mu_{\rm B}} \approx B_0 S_z + A_0 S_z I_z + \frac{A_0}{2}\left(S_+ I_- + S_- I_+\right) \tag{2}$$

gives the Zeeman energy for each nuclear spin multiplet m_I. The resonance condition of the HFS spectra with the Zeeman energy splittings $\Delta E(m_I)$ is given by[31]

$$\frac{\Delta E(m_I)}{g\mu_{\rm B}} = B_0 + A_0 m_I + \frac{1}{2}\left(\frac{A_0^2}{B_0}\right)(I(I+1) - m_I^2). \tag{3}$$

The second term ($\propto m_I$) predicts equally spaced $2I + 1 = 6$ peaks for $I = 5/2$, corresponding to each m_I value. The third term ($\propto m_I^2$) provides a linear deviation from the equally spaced peak separation on m_I as a higher order effect of the hyperfine interaction. For the center two peaks with $m = +\frac{1}{2}$ and $-\frac{1}{2}$, the third term is the same as each other. Thus, the center splitting $\left(\Delta E(\frac{1}{2}) - \Delta E(-\frac{1}{2})\right)/g\mu_{\rm B}$ is A_0 (G), which is 96.2 (G) for Mn-DNA.

The parameter A_0 reflects the ionicity of Mn bonding with surrounding atoms, as demonstrated in Table 1 for the Ca-host case. For the Mn ions with ionic bonding in CaF_2 matrix, $A_0 \approx 100$ G, but in CaS with increased covalent nature, A_0 reduces down to 80 G. Covalent bonding has directionally extended wavefunctions to outside, which reduces the electron charge density at the nucleus, that is, the hyperfine interaction. If one compares $A_0 = 96$ G for the Mn in $(Ca_{1-x}Mn_x)$-DNA with the average value of $A_0 = 98$ G for the Mn substituted

Table 1. Hyperfine coupling constant of Mn^{2+} ions embedded in the calcium halides and chalcogenides, in the unit of G.[30,32] The linear relationship $g\mu_{\rm B}A_0 = 19.4 + 83.3\ i$ [10^{-4}cm^{-1}] or $A_0 = 20.8 + 89.2\ i$ [G] has been estimated from the calculated result based on the experimental data set, where i is the degree of ionic character.[32] Here, note that the slope depends on the host ion species. To convert from G to cm^{-1}, divide by 1.071×10^4 [G/cm^{-1}].

Host	CaF_2	CaO	$CaCl_2$	CaS
A_0 (G) for Mn^{2+}	101	91.8	91.1	81.1
Bonding nature	ionic	$\Longleftrightarrow$	covalent	

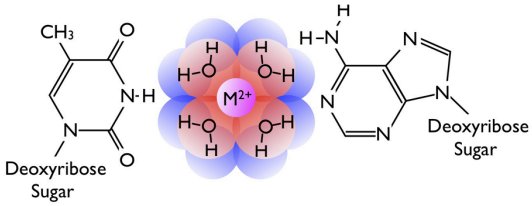

Figure 3. A schematic model for M-DNA.[30] The metal ion is surrounded by the several water molecules in between, for example, thymine and adenine, in place of hydrogen bondings in natural DNA. This model is based on the following three points; (1) the present result of ionic bonding character, (2) the known fact that the metal ions prefer to form a direct covalent bond with nitrogen and (3) the recent observations of M-DNA by STM, showing some ring around the metal ion in between the bases. In a solution, a lot of water molecules more than these in this Figure would fill the space around the bases and would make rapid exchange with each other.

dilutely in several ionic fluorides such as LiF, NaF, KF, MgF_2 and CaF_2, it is reasonable to conclude that the bonding of the Mn ion in DNA is of purely ionic, that is, the wavefunctions are spherically symmetric. Figure 3 shows a schematic model for the Mn^{2+} ion hydrated by the several water molecules in between the bases of a base pair. This model meets the requirement of the present conclusion that the metal ion should be isolated from the nitrogen, since they tend to form covalent bondings. It is evident that the ionic bonding modifies the electronic states of DNA very little.

3.2 Observation of M-DNA by STM

There is a long history to try to observe DNA directly by STM (Scanning Tunneling Microscopy) after the invention of the STM technique by Binnig and Rohrer and coworkers.[33] We have started a try to observe DNA with STM, keeping in mind its very high difficulty to realize, because of mimic helical structures on HOPG surface,[34,35] and very low, almost zero possibility to resolve metal ions of M-DNA. As a reference, we have measured natural DNA at first with easyScan2 by Nanosurf.

The presence of DNA strands are easily confirmed with AFM, which can reflect actual dimension only in hight, but not the width of images, which is dominated by the tip diameter. Without dipping a HOPG substrate into a DNA solution, nothing like wires could be found with AFM. After dipping into an aqueous solution with appropriate DNA concentration, we could find a long straight wire with a height of 2 nm, consistent with DNA double helix.

Thus, we tried to apply STM. A lot of different images were found, like double helix structure, bundles, some of which could be mimic DNA. Occasionally flat-ladder images with definite dimensions; 2 nm in separation of two DNA backbones, consistent with the diameter of double helical DNA, 0.7 nm of periodicity along DNA

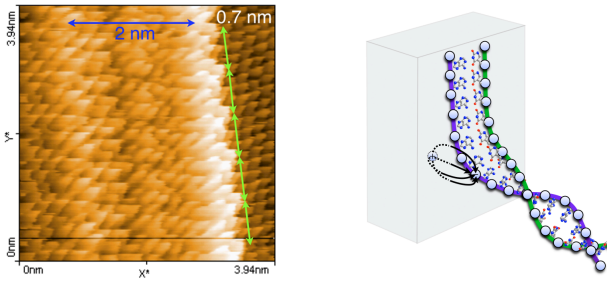

Figure 4. (Left) An example of STM images of the salmon DNA (Wako) with a novel flat-ladder form on HOPG (highly oriented pyrolytic graphite) substrate.[29] (Right) A model for the formation of a flat-ladder DNA on a conducting substrate like HOPG when lift up the HOPG substrate from a dilute DNA aqueous solution.

backbone, also consistent with the unit length of DNA backbone (DNA step height of 0.34 nm divided by sin(35°) ≈ 0.68 nm), as demonstrated in Fig. 4. In natural salmon DNAs, several examples with similar measurements were found, so far. In the right of Fig. 4, the possible mechanism for the ladder form are schematically illustrated: Positive image charge for PO_4^- is induced in the opposite side at the equidistance against the HOPG conducting surface. They attract each other and finally PO_4^- ion fixed on the HOPG surface with the image charge. Here, it is noteworthy that the DNA backbones of a double helix run to the opposite direction to each other. Thus, the two backbones of a flat ladder form of DNA should provide different images from each other in form and brightness.

In the metal incorporated DNAs, clear images for the ladder form of Mn-DNA and Co-DNA with two nicely periodic DNA backbones, bases and metal ions were found. The separation of the backbones in Mn-DNA are 2.6 nm, which is larger than 2.0 nm for salmon DNA, because of the additional ring image with a center dot (Ring-dot image) located periodically at the center part in between the bases of the ladder form. The ring-dot images are well correspond to the hydrated Mn ions in Fig. 3 in size and location. The repeat distance along the DNA backbone is ≈ 0.8 nm, which is also larger than 0.7 nm for the salmon DNA. In Co-DNA, the separation of backbones is 2.4 nm and repeat distance is 0.7 nm, both of which are larger than that of salmon DNA, but smaller than that of Mn-DNAs, suggesting some difference of the hydrated metal ion structure for Mn-DNA and Co-DNA. Thus, the model structure in Fig. 3 is also supported by the STM study in M-DNAs. Details will be published elsewhere.

4. ELECTRONIC STATES OF M-DNA

The electronic states of M-DNAs prepared by the ethanol-precipitation technique have been established in the viewpoint of magnetic properties and the optical absorption.[21,24,29,30] In most of the M-DNAs, Na cations as counter ions for PO_4^- anions in the DNA backbones are simply replaced by the divalent metal ions, M^{2+}, which locate in between the bases of a base pair. Thus, the electronic states of DNA are unchanged with M^{2+} incorporation to DNA, as confirmed by ESR and optical absorption. Only the exception is Fe-DNA. Fe-DNA prepared with $FeCl_2$ and DNA aqueous solution has transformed into Fe^{3+}-DNA. Additional optical absorption of Fe^{3+}-DNA shows the same absorption profiles as that of $Fe^{3+}Cl_3$. However, $Fe^{3+}O(OH)$ resulted from hydrolysis + oxidation shows definite shifts from that of $Fe^{3+}Cl_3$. These findings suggest that Fe^{3+} has spherical wavefunctions with ionic character, as same as Mn-DNA, and that the valence change to Fe^{3+} is due to the reaction of Fe^{2+} and DNA, but not hydrolysis + oxidation.

4.1 Magnetic Properties

In M-DNAs with M=Mg, Ca, Zn, it has been confirmed that no intrinsic ESR signals related to M^{2+} were observed.[21–24,29] Since M^{2+} ions have only closed electron shells, absence of ESR signals is the clear evidence that the electronic states of these metal ions are divalent in M-DNA. This fact suggests that M^{2+} acts as counter ions for two PO_4^- anions in place of two Na^+ cations, that is, the ion exchange reaction. Thus, the electronic states of DNA are unchanged after incorporation of M^{2+}. This conclusion is consistently supported by the optical absorption study.

In Mn-DNA, ESR signal of five $3d$-electrons in Mn^{2+} is observed, as demonstrated in Fig. 2. The spectrum shape shows characteristic features, depending on the isomeric form of Mn-DNA, A-form or B-form. The B-form DNA is stable in humid conditions and shows the line shape intermediate between Lorentzian and Gaussian, because of the one dimensional (1D) correlation of the exchange interaction between Mn ions.[21,24,29] On the other hand, the A-form Mn-DNA in dry conditions provides 1D but a spiral Mn ion array, which can interact three dimensionally with the spiral Mn arrays of the neighboring A-form Mn-DNAs. As a result, three dimensional exchange correlation causes Lorentzian ESR line shape.[21,29] The magnetization curve at 2 K in Mn-DNA is also reproduced very well with the Brillouin function of $S = \frac{5}{2}$ independent of isomeric forms. In aqueous solution of Mn-DNA, a six hyperfine split signal is observed, which gives important information on the bonding nature of Mn ions, as discussed in §3.1.

In Fe-DNA, the sample color is typical of Fe^{3+}, ocher, as demonstrated in Fig. 5.[29] The strict confirmation of the Fe valence is g-shift of ESR signal; Fe^{3+} has five $3d$ electrons, as same as Mn^{2+}, ESR signal will appear at the free electron g value, $g = 2$. In contrast, since Fe^{2+} has six d electrons with $S = 2$ and $L = 2$, g-value should be

Figure 5. Left: $FeCl_3$, Center: $FeCl_2$, Right: Fe-DNA. Fe-DNA was prepared from the aqueous solution of $FeCl_2$ and DNA.

complicated by crystal fields.[31] Fe-DNA actually gave ESR signal at $g = 2$, as expected for Fe^{3+}.[21,24,29] Here, it is important to confirm that these Fe^{3+} resulted from the reaction of Fe^{2+} with DNA, but not unexpected hydrolysis + oxidation process, as will be discussed in §4.2.

The issue to be solved is where the electron transferred from Fe^{2+}. One possible candidate is the base π band. In this case, ESR from π-electron might be observed around $g \approx 2$. The observed ESR signal is composed of 3 components to reproduce the spectra successfully.[21] On the other hand, the electrical conductivity did not show any enhancement over B-DNA, which suggests the presence of the strong electron-electron correlation effect in the baes π-electron band.

4.2 Optical absorption

One of the basic parameters, optical absorption has been studied in aqueous solution of M-DNA. On the basis of the conclusions mentioned above, usual divalent metal ions in M-DNA are ineffective to modify the electronic states of DNA, such as charge injection to DNA. Actually, the optical absorption spectra for the aqueous solution of M-DNA (M=Mg, Ca, Mn) are quite similar to that of the DNA aqueous solution; the definite semiconducting energy gap of more than 4 eV, as shown in Fig. 6.

Only the exception is Fe-DNA, where Fe^{2+} transforms to Fe^{3+} in Fe-DNA (§4.1). Characteristic features of optical absorption in the Fe-DNA solution are the suppression of interband absorption and the tail into the energy gap. One possible reason why the interband absorption could be suppressed is due to the filling of π^* band of the nucleobases by the charges transferred from Fe^{3+} in Fe-DNA.

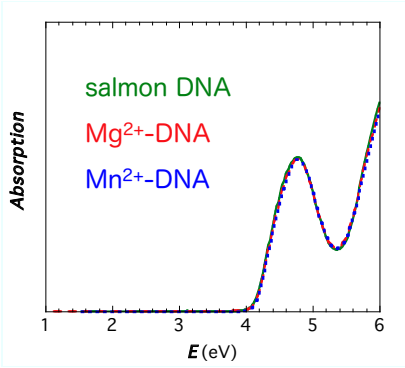

Figure 6. UV/VIS absorption spectrum of the salmon-DNA (Wako) in aqueous solution, together with Mg-DNA and Mn-DNA solutions. Three curves for these samples agree quite well with each other, consistent with the ion exchange process.

4.2.1 Formation mechanism of Fe^{3+}

To unveil the creation mechanism of Fe^{3+} in Fe-DNA, optical absorption spectra of $FeCl_3$ and FeO(OH) were investigated in Fig. 7, where FeO(OH) is a reaction product of $FeCl_2$ by hydrolysis + oxidation. We can easily discriminate two Fe^{3+} species with the definite red shift of FeO(OH) spectrum against that of $FeCl_3$. However, FeO(OH) is substantially produced only at elevated temperatures, for example, 50°C for 2 hours. As the mixture

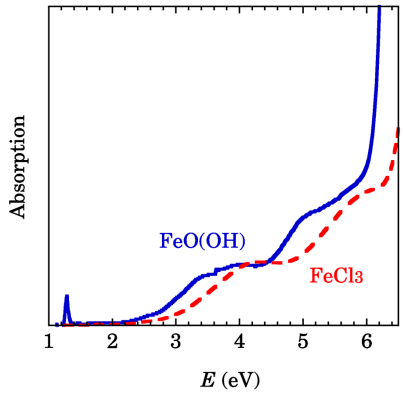

Figure 7. Optical absorption spectra in $Fe^{3+}Cl_3$ and $Fe^{3+}O(OH)$ aqueous solutions. FeO(OH) was prepared with $FeCl_2$ aqueous solution for 2 hours at 50°C and the intensity was multiplied by 10 to compare with $FeCl_3$. Note the red shift of FeO(OH) spectrum from $FeCl_3$, reflecting the difference of the electronic states, covalent bond in FeO(OH) and spherical ionic wavefunctions in $FeCl_3$. Additional optical absorption caused by Fe incorporation in Fe-DNA solution has the same spectrum as that in $FeCl_3$, indicating Fe^{3+} has an ionic nature with spherical wavefunctions in Fe-DNA.

of DNA with $FeCl_2$ gradually transforms into Fe-DNA with time, the additional absorption as same as that of $FeCl_3$ grows. Figure 8 shows the time evolution of Fe^{3+} creation at room temperature in the three different cases from bottom to top; 1) $FeCl_2$ solution, 2) poly(dA-dT) + $FeCl_2$ solution, and 3) poly(dG-dC) + $FeCl_2$ solution. As clearly demonstrated in Fig. 8, $FeCl_2$ aqueous solution is sufficiently stable in air at room temperature, indicating that the oxidation of Fe^{2+} caused by air is safely neglected in the present sample preparation. The fact that the linear increase of Fe^{3+} intensity happens only with the presence of DNA, is a clear evidence for the reaction of Fe^{2+} with DNA, accompanied by the charge transfer from Fe^{2+} to DNA.

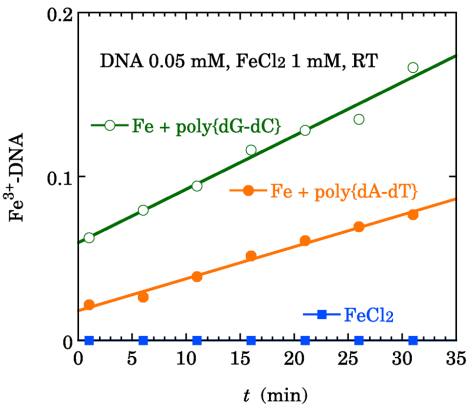

Figure 8. The time evolution of the relative intensity of ionic Fe^{3+} ions. The solid square: $FeCl_2$ aqueous solution, the solid circle: $FeCl_2$ + poly(dA-dT) aqueous solution and the open circle: $FeCl_2$ + poly(dG-dC) aqueous solution. Origo DNAs are 30mer. FeO(OH) formation in $FeCl_2$ aqueous solution can be neglected at least for 30 min at room temperature. DNA is inevitable for the formation of Fe^{3+} in aqueous $FeCl_2$ solution.

4.3 Alternative electronic states of M-DNA

Recently, Omerzu and coworkers have reported new results on Zn-DNA by a special sample preparation with a freeze-dry technique.[28] They report that ESR intensity behave as almost temperature independent, like Pauli

susceptibility in the usual metals, that is, the strongly correlated electron systems. However, they reported that the valence of Zn ion is divalent, that is, ESR silent. Thus, the origin of the Pauli-like ESR signal is an open question. We tried to reproduce their result several times, but it is not successful, yet. Anyway, their result suggests a possibility of the other electronic states of Zn ions.

Since the freeze-dry method forces to remove water molecules from the samples, one possible difference is the number of water molecules in Zn-DNA. The ethanol-precipitation method resulted in incorporation of hydrated metal ions in between the bases of a base pair. If the freeze-dry method could remove hydrated water molecules, Zn ion would form the covalent bondings with nitrogen atoms in the bases, which can definitely modify the electronic states of Zn-DNA. The investigation is in progress to confirm this possibility.

5. SUMMARY

The electronic states of the metal-incorporated DNAs were studied from the viewpoint of the structure, magnetism and optical absorption. ESR spectrum of Mn-DNA aqueous solution shows six hyperfine split peaks, which reflects the information on the bonding nature of Mn ion; highly ionic in Mn-DNA. This conclusion of bonding nature suggests that the metal ion is hydrated by several water molecules in between the bases of a base pair. This requirement was due to the preference of metal ions to form the covalent bond with nitrogen atoms of a base pair and was consistent with the STM images of M-DNAs.

In most of the M-DNAs, the valence of M is two, corresponding to the simple ion exchange by M^{2+} in place of two Na^{+} counter cations for tow PO_4^{-} anions. As a result, negligible modification of the electronic states of DNA has occurred, consistent with almost the same optical absorption spectra of natural DNA and M-DNAs. Only the exception is the Fe-DNA, where Fe^{2+} was transformed to Fe^{3+} with charge transfer to DNA.

Recent report by Omerzu and coworkers proposed possible alternative electronic states of Zn ions in Zn-DNA prepared by a freeze-dry method. A possible candidate of the electronic states would be the covalent bonding of Zn ions with the nitrogen atoms of the bases under the extremely dried condition.

ACKNOWLEDGMENTS

This report is the review article based on the collaboration with many students in the ESR subgroup, Dept. of Physics, Tokyo Metropolitan University from 2002. The author would like to thanks Dr. Kodama for his support in the UV/VIS measurements. This work is supported in part by JSPS KAKENHI (C) (22540371).

REFERENCES

[1] Watson, J. D. and Crick, F. H., "Molecular structure of Nucleic Acid," Nature 171, 737-738 (1953).

[2] Wilkins, M. H. F., Stokes, A. R. and Wilson, H. R., "Molecular structure of deoxypentose nucleic acids," Nature 171, 738-740 (1953).

[3] Franklin, R. E. and Gosling, R. G., "Molecular configuration in sodium thymonucleate," Nature 171, 740-741 (1953).

[4] Bowater, R. P. "DNA structure" in Nature Encyclopedia of the human genome (ed. Cooper, D. M.), Macmillan, 1-9 (2003).

[5] Fink, H.-W. and Schenenberger, C., "Electrical conduction through DNA molecules," Nature 398, 407-410 (1999).

[6] de Pablo, P. J., Moreno-Herrero, F., Colchero, J., Gomez Herrero, J., Herrero, P., Baro, A. M., Ordejon, P., Soler, J. M. and Artacho, E., "Charge transport in DNA," Phys. Rev. Lett. 85, 4992 (2000).

[7] Porath, D., Bezryadin, A., Vries, S. d. and Dekker, C., "Direct measurement of electrical transport through DNA molecules," Nature 403, 635-638 (2000).

[8] Tran, P., Alavi, B. and Gruner, G., "Charge transport along the λ-DNA double Helix," Phys. Rev. Lett. 85, 1564-1567 (2000).

[9] Iguchi, K., "Semiconductivity and band gap of a double strand of DNA," J. Phys. Soc. Jpn. 70, 593-597 (2001).

[10] Kasumov, A. Y., Kociak, M., Gueron, S., Reulet, B., Volkov, V. T., Klinov, D. V. and Bouchiat, H., "Proximity-induced superconductivity in DNA," Science 291, 280-282 (2001).
[11] Zhang, Y., Austin, R. H., Kraeft, J., Cox, E. C. and Ong, N. P., "Insulating behavior of λ-DNA on the micron scale," Phys. Rev. Lett. 89, 198102-198101-198104 (2002).
[12] Ventra, M. D. and Zwolak, M. "DNA Electronics" in Encyclopedia of Nanoscience and Nanotechnology (ed. Nalwa, H. S.), American Scientific Publishers, Valencia, 1-19 (2004).
[13] Shih, W. M., Quispe, J. D. and Joyce, G. F., "A 1.7-kilobase single-stranded DNA that folds into a nanoscale octahedron," Nature 427, 618-621 (2004).
[14] Dekker, C. and Ratner, M. A., "Review of DNA physics," Phys. World 14, 29 (2001).
[15] Wettig, S. D., Li, C.-Z., Long, Y.-T. and Kraatz, H.-B., "M-DNA: a self-assembling molecular wire for nanoelectronics and biosensing," Analytical Sciences 19, 23-26 (2003).
[16] Endres, R. G., Cox, D. L. and Singh, R. R. P., "Colloquium: The quest for high-conductance DNA," Rev. Mod. Phys. 76, 195-214 (2004).
[17] Yu, Z. G. and Song, X., "Variable range hopping and electrical conductivity along the DNA double helix," Phys. Rev. Lett. 86, 6018 (2001).
[18] Mizoguchi, K., Tanaka, S., Ogawa, T., Shiobara, N. and Sakamoto, H., "Magnetic study of the electronic states in B-DNA and M-DNA doped with metal ions," Phys. Rev. B 72, 033106, (033101-033104) (2005).
[19] Nakamae, S., Cazayous, M., Sacuto, A., Monod, P. and Bouchiat, H., "Intrinsic Low Temperature Paramagnetism in B-DNA," Phys. Rev. Lett. 94, 248102 (2005).
[20] Lee, J. S., Latimer, L. J. P. and Reid, R. S., "A cooperative conformational change in duplex DNA induced by Zn^{2+} and other divalent metal ions," Biochem. Cell Biol. 71, 162-168 (1993).
[21] Mizoguchi, K., Tanaka, S., Ojima, M., Sano, S., Nagatori, M., Sakamoto, H., Yonezawa, Y., Aoki, Y., Sato, H., Furukawa, K. and Nakamura, T., "AF-like Ground State of Mn-DNA and Charge Transfer from Fe to Base-π-Band in Fe-DNA," J. Phys. Soc. Jpn. 76, 043801-043801-043804 (2007).
[22] Mizoguchi, K., "EPR study of the electronic states in natural and doped DNA" in International Conference of Electroactive Polymers 2004 (ICEP04), Allied Publishers, Dalhausie, India, 1-10 (2007).
[23] Mizoguchi, K., Tanaka, S. and Sakamoto, H., "Electronic States of natural and metal-ion doped DNAs," J. Low Temp. Phys., 142, 379-382 (2007).
[24] Mizoguchi, K., "Physical properties of natural DNA and metal ion inserted M-DNA," Proc. SPIE 7040, 70400Q (70401-70409) (2008).
[25] Matsui, H., Toyota, N., Nagatori, M., Sakamoto, H. and Mizoguchi, K., "Infrared spectroscopic studies on incorporating the effect of metallic ions into a M-DNA double helix," Phys. Rev. B 79, 235201 (2009).
[26] Rakitin, A., Aich, P., Papadopoulos, C., Kobzar, Y., Vedeneev, A. S., Lee, J. S. and Xu, J. M., "Metallic Conduction through Engineered DNA: DNA nanoelectronic building blocks," Phys. Rev. Lett. 86, 3670-3673 (2001).
[27] Alexandre, S. S., Soler, J. M., Seijo, L. and Zamora, F., "Geometry and electronic structure of M-DNA (M = Zn^{2+}, Co^{2+}, and Fe^{2+})," Phys. Rev. B 73, 205112 (205111-205115) (2006).
[28] Omerzu, A., Anzelak, B., Turel, I., Strancar, J., Potocnik, A., Arcon, D., Arcon, I., Mihailovic, D. and Matsui, H., "Strong Correlations in Highly Electron-Doped Zn(II)-DNA Complexes," Phys. Rev. Lett. 104, 156804 (2010).
[29] Mizoguchi, K., "Electronic states of M-DNA incorporated with divalent metal ions," Proc. SPIE 7765, 77650R (77651-77612) (2010).
[30] Nagatori, M., Ojima, M., Ibuki, Y., Sakamoto, H. and Mizoguchi, K., "Electronic states of metal ions incorporated in Mn-DNA," J. Phys. Soc. Jpn., in press. (2011).
[31] Abragam, A. and Bleany, B. Electron Paramagnetic Resonance of Transition Ions (Clarendon Press, Oxford, 1970).
[32] Zhitomirskii, A. N., "Relationship between the degree of ionic character of a bond and the EPR hyperfine coupling constant for monotypal binary crystals doped with manganese," Journal of Structural Chemistry 9, 532-535 (1968).
[33] Binnig, G., Rohrer, H., Gerber, C. and Weibel, E., "Surface Studies by Scanning Tunneling Microscopy," Phys. Rev. Lett. 49, 57 (1982).

[34] Clemmer, C. R. and Thomas P. Beebe, J., "Graphite: A mimic for DNA and other biomolecules in scanning tunneling microscope studies," Science 251, 640-642 (1991).

[35] Heckl, W. M. and Binnig, G., "Domain walls on graphite mimic DNA," Ultramicroscopy 42, 1073-1078 (1992).